

# Synchronization of Multiple Videos

Avihai Naaman<sup>\*1,2</sup>, Ron Shapira Weber<sup>\*1,2</sup>, and Oren Freifeld<sup>1,2,3</sup>

<sup>1</sup>Department of Computer Science, Ben-Gurion University of the Negev (BGU)

<sup>2</sup>Data Science Research Center, BGU. <sup>3</sup>School of Brain Sciences and Cognition, BGU.

## Abstract

*Synchronizing videos captured simultaneously from multiple cameras in the same scene is often easy and typically requires only simple time shifts. However, synchronizing videos from different scenes or, more recently, generative AI videos, poses a far more complex challenge due to diverse subjects, backgrounds, and nonlinear temporal misalignment. We propose Temporal Prototype Learning (TPL), a prototype-based framework that constructs a shared, compact 1D representation from high-dimensional embeddings extracted by any of various pretrained models. TPL robustly aligns videos by learning a unified prototype sequence that anchors key action phases, thereby avoiding exhaustive pairwise matching. Our experiments show that TPL improves synchronization accuracy, efficiency, and robustness across diverse datasets, including fine-grained frame retrieval and phase classification tasks. Importantly, TPL is the first approach to mitigate synchronization issues in multiple generative AI videos depicting the same action. Our code and a new multiple video synchronization dataset are available at <https://bgu-cs-vil.github.io/TPL/>*

## 1. Introduction

Multiple Video Synchronization (MVS) of the same action is a challenging problem in computer vision, particularly in unconstrained settings. Standard solutions often rely on pairwise alignment [2, 8, 15, 32], where each pair of videos is matched in isolation. Although such methods are relatively straightforward for small-scale problems, they suffer from two major shortcomings when extended to multiple videos. The first is the high computational cost. Consider a dataset of  $N$  videos, each containing  $L$  frames, alongside a new video of length  $L$  for synchronization or frame retrieval. In a pairwise approach, every frame must be compared against all  $N \times L$  frames in the training set, incurring an  $O(N \times L^2)$  complexity. This exhaustive nearest-neighbor (NN) search is prohibitively expensive for real-world scenarios, where both  $N$  and  $L$  can be large.

The second is the lack of global consistency. Even if pairwise alignments yield accurate matches in isolation, they do not necessarily guarantee a *joint* alignment across the

entire collection of videos. Repeated pairwise matches can conflict, since different pairs may learn disparate references for similar action phases. As a result, there is no unified representation of the action progression that consistently aligns *all* videos.

To address these issues, we advocate a **prototype-based** alignment strategy that bypasses the need for a single reference video and enables the synchronization of *all* videos at once. We propose **Temporal Prototype Learning (TPL)**, which learns one-dimensional ‘bottleneck’ signals capturing the underlying temporal structure (*i.e.*, action prototypes) as universal anchors. By mapping each frame in every video to a shared temporal axis, TPL ensures global consistency and drastically reduces the computational cost. Synchronizing or retrieving a specific phase at time step  $t$  for a new video thus amounts to referencing the  $t$ -th point in the learned prototype, rather than searching through the entire dataset. [Figure 1](#) illustrates the TPL framework, where multiple videos are mapped to the same prototype space. Our main contributions are:

- **Prototype-Based Synchronization:** We introduce a novel approach to jointly align multiple videos via a shared prototype space, overcoming the scalability and consistency challenges of pairwise methods.
- **Diffeomorphic Multitasking Autoencoder (D-MTAE):** A novel architecture for learning one-dimensional ‘bottleneck’ representation from multivariate video embeddings. D-MTAE can be trained on any pretrained video feature extractor and enables fast inference and robust multiple alignment.
- **Linear-Time Frame Retrieval:** since, after alignment, semantically similar frames are mapped to the same time point, frame retrieval simply entails returning all frames at that time point.
- **Synchronization of GenAI videos:** We show that TPL can sync not only multiple real-world videos but also multiple AI-generated videos depicting the same action. To demonstrate this, we also generated and annotated (for evaluation purposes only) the first GenAI-MVS dataset.

## 2. Related Work

**Video Representation Learning.** Several approaches leverage sequence-level or pairwise matching signals to

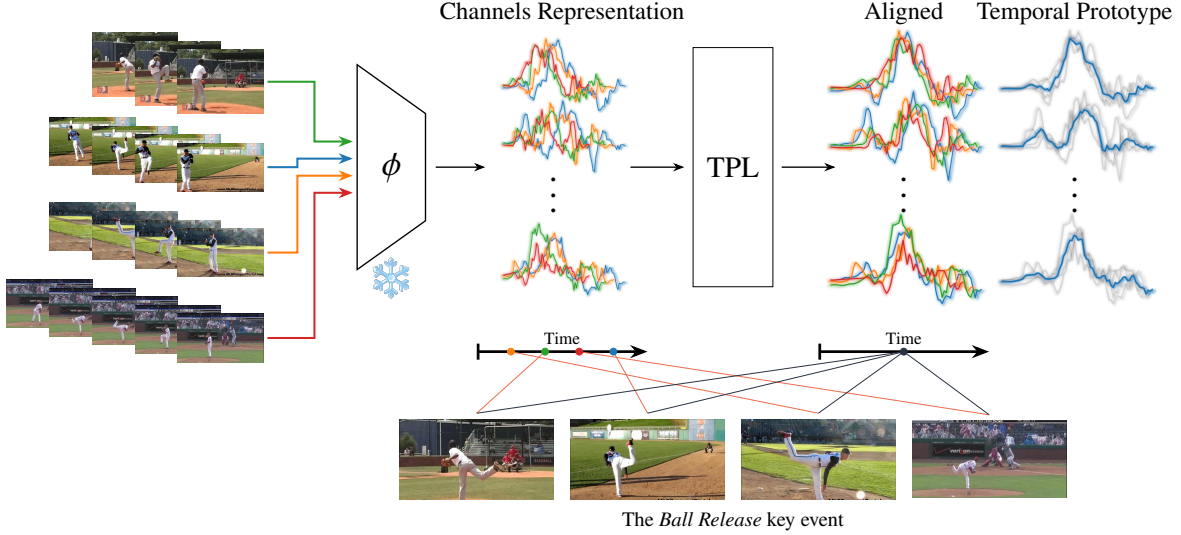


Figure 1. **Temporal Prototype Learning (TPL)** uses an ‘off-the-shelf’ feature extractor, denoted by  $\phi$ , to generate initial multichannel action progression sequences for videos of the same action (e.g., Ball pitch [33]). Colors indicate different (and temporally-misaligned) videos of the same action. TPL produces the joint alignment and prototypical sequence, mapping key events (e.g., *Ball Release*)

learn representations from videos. TCC [8] focuses on local alignment across pairs of videos, while GTA [11] extends this to longer sequences via a relaxed DTW-based contrastive loss. LAV [12] introduces additional regularization to avoid trivial solutions, and VAVA [15] allows variations in action order using priors on the optimal transport matrix. CARL [2] adopts a transformer-based contrastive framework with spatial and temporal augmentations. Although these methods have demonstrated success in pairwise settings, scaling them to large collections of videos typically requires extensive nearest-neighbor (NN) searches, which is computationally demanding and memory-intensive. In parallel, large-scale pretrained image models such as DINO [1] or OpenCLIP [3] can be used for videos by extracting the [CLS] token or feature vector from each frame. Stacking these tokens over time yields a sequence of embeddings that capture both spatial semantics (from the pretrained image model) and temporal information (through the ordering of frames). We show TPL can use these embeddings for synchronizing multiple videos.

**Time-Series Alignment.** Classical time-series alignment algorithms such as Dynamic Time Warping (DTW) [22, 23] and SoftDTW [4] are widely used to find optimal, order-preserving alignments between a pair of temporal sequences. SoftDTW, in particular, offers a differentiable variant, which has enabled end-to-end training when coupled with neural network feature extractors. However, these methods have a quadratic complexity in both time and memory w.r.t. sequence length, limiting their scalability.

**Prototype Learning and Temporal Prototypes.** Prototype learning has proven effective in few-shot learning scenarios [29], where prototypical representations facilitate robust classification with minimal labeled data. In principle, a *temporal* prototype can serve a similar role for video alignment, essentially summarizing the action progression into a single sequence. DTW Barycenter Averaging (DBA) [19, 20] and SoftDTW barycenters (SoftDBA) [4] offer ways to compute an average sequence under their respective distance function. Diffeomorphic Temporal Alignment Net (DTAN) [16, 26, 27] learns diffeomorphic warping functions [9, 10], effectively jointly aligning all input sequences to their average. Although DTAN enables end-to-end learning of joint alignment (JA), it was not developed for aligning high-dimensional *video embeddings* with large variation in length. In this work, we show how TPL addresses these issues.

**Multiple Video Synchronization: Limitations and Gaps.** While pairwise alignment and small-scale joint alignment approaches have made significant progress, critical gaps remain for large-scale, *multi-video* synchronization. First, naively extending pairwise methods to  $N$  videos often leads to  $O(N \times L^2)$  complexity in retrieval or synchronization, posing severe scalability constraints. Second, aligning pairs independently does not guarantee a *globally-consistent* representation across all videos. Previous multiple video synchronization (MVS) methods focus on well-behaved scenarios that mainly involve multiple cameras recording the same scene, where the misalignment can be explained by a simple translation [14, 28, 31]. However, synchronizing different scenes requires nonlinear alignment of the time axis.

Table 1. Table of notations.

| Symbol                      | Description  |
|-----------------------------|--|
| $S_i$                       | $i$ -th video.   |
| $s_t^i$                     | Frame $t$ of video $S_i$ .                                 |
| $u_t^i = \phi(s_t^i)$       | Per-frame embedding.                                       |
| $U_i = \{u_t^i\}_{t=1}^L$   | Embedded feature sequence, $\in \mathbb{R}^{C \times L}$ . |
| $\tilde{U}_i$               | Reconstructed embedded sequence.                           |
| $\theta_i \in \mathbb{R}^d$ | Predicted warp parameters for $U_i$ .                      |
| $T^{\theta_i}$              | Parametric time-warp associated with $\theta_i$ .          |
| $Z_i$                       | Univariate representation.                                 |
| $\tilde{U}/\hat{Z}$         | Average aligned sequence.                                  |

In this paper, we propose a new framework, called *Temporal Prototype Learning (TPL)*, that addresses the limitations of existing approaches by jointly aligning multiple videos in a single, shared prototype space. This design enables robust synchronization, eliminates the need for exhaustive nearest-neighbor searches, and yields a linear-time retrieval mechanism for new video sequences.

### 3. Method

We propose a novel approach for the synchronization of multiple videos without a reference. Our goal is to map similar action sequences to the same time step w.r.t. the action progression. To achieve this, we introduce TPL, which involves performing simultaneous dimensionality reduction and JA in the embedded space using a novel D-MTAE (Figure 2 depicts the framework). This section is organized as follows. We first review the required preliminaries in § 3.1. In § 3.2, we present a detailed explanation of the TPL framework, including its modules and loss functions. In § 3.3, we describe how to perform MVS and annotation transfer with TPL. Lastly, we discuss the limitations of TPL § 3.4.

#### 3.1. Preliminaries

**Notation and Setup (see Table 1).** Consider  $N$  videos,  $(S_i)_{i=1}^N$ . Let  $S_i = (s_1^i, s_2^i, \dots, s_L^i)$  be a video of length  $L$ , where  $s_t^i$  is the  $t$ -th frame. We define the per-frame embedding  $u_t^i = \phi(s_t^i) \in \mathbb{R}^C$ , where  $\phi$  is a feature extractor and  $C$  is the number of channels (*i.e.*, the embedding dimension) of the representation of the video. The embedded feature sequence is  $U_i = \{u_t^i\}_{t=1}^L \in \mathbb{R}^{C \times L}$ . Thus, the set of video embeddings to be synchronized is  $\{U_i\}_{i=1}^N$ .  $U_i$  could either be produced by applying an image-based classifier (*i.e.*, the DINO [CLS] token [1]) to each frame or a video-based one such as CARL [2]. For each  $U_i$ , we denote the predicted warping parameters and the corresponding time warp as  $\theta_i \in \mathbb{R}^d$  and  $T^{\theta_i}$  respectively, such that  $U_i \circ T^{\theta_i}$  is the warped sequence and  $T^{\theta_i}$  belongs to a  $d$ -dimensional parametric transformation family. Finally, the average of the temporally-aligned sequences is  $\hat{U} = \frac{1}{N} \sum_{i=1}^N U_i \circ T^{\theta_i}$ .

The Joint Alignment (JA) problem can then be thought of

as finding the set of warping parameters between  $\{U_i\}_{i=1}^N$  and  $\hat{U}$  which minimize their discrepancy,  $D$  (*e.g.*, the Euclidean distance). Since  $\hat{U}$  is unknown, the JA problem becomes:

$$(T^{\theta_i})_{i=1}^N, \mu = \arg \min_{(T^{\theta_i})_{i=1}^N \in \mathcal{T}, U} \sum_{i=1}^N D(U, U_i \circ T_i) \quad (1)$$

where  $(T^{\theta_i})_{i=1}^N$  and  $\mu$  denote the optimal warping parameters and average sequence, respectively, and  $\mathcal{T}$  is the transformation family (*e.g.*, phase-shift, elastic, *etc.*). Partly due to the unsupervised nature of the task, a regularization term is usually added to avoid trivial solutions and/or unrealistic deformations. The problem is then reformulated as:

$$(T^{\theta_i})_{i=1}^N, \mu = \arg \min_{(T^{\theta_i})_{i=1}^N \in \mathcal{T}, U} \sum_{i=1}^N D(U, U_i \circ T_i) + \mathcal{R}(T^{\theta_i}; \lambda) \quad (2)$$

where  $\mathcal{R}(T^{\theta_i}; \lambda)$  is the regularizer over  $T^{\theta_i}$ , and  $\lambda$  is a hyperparameter (HP) controlling the regularization strength. An important, yet often overlooked, fact is that  $\lambda$  is usually dataset specific, must be found via an expensive search, and that finding a good value requires supervision (*i.e.*, ground-truth labels are needed to rank the performance with different values of  $\lambda$ ). To alleviate this issue, we follow a regularization-free approach [26] to JA which uses the Inverse-Consistency Averaging Error (ICAE; detailed below),

#### Diffeomorphic Temporal Alignment Nets (DTAN).

DTAN [16, 26, 27] is a learning-based model designed for time series JA. Given  $N$  sequences  $\{U_i\}_{i=1}^N$ , DTAN predicts a set of continuous time-warp parameters  $\{\theta_i\}_{i=1}^N$  to minimize the within-class variance. This is akin to finding the average sequence. These warps are applied via CPAB transformations [9, 10] (described below). DTAN has been designed for *univariate* time series and was evaluated on the relatively ‘well-behaved’ UCR archive [5]. While DTAN could arguably be generalized to multivariate representations of videos, applying a single warp to each multivariate sequence can overlook channel-specific temporal variations that, in turn, hinder the average sequence’s computation. Another limitation specific to ICAE is that the JA of variable-length multivariate data (as opposed to variable-length univariate data) usually results in a ‘shrinking’ effect, where the average sequence length is much shorter than the original data.

Our proposed TPL resolves these issues by 1) introducing a univariate ‘bottleneck’ that discards channel-specific variations not shared across all sequences, and 2) setting the average sequence to match the median length of the data. This design allows for robust JA in the high-dimensional embedding space while retaining the desirable properties of DTAN. That is, end-to-end, misalignment-invariant learning of a shared temporal structure across multiple videos.

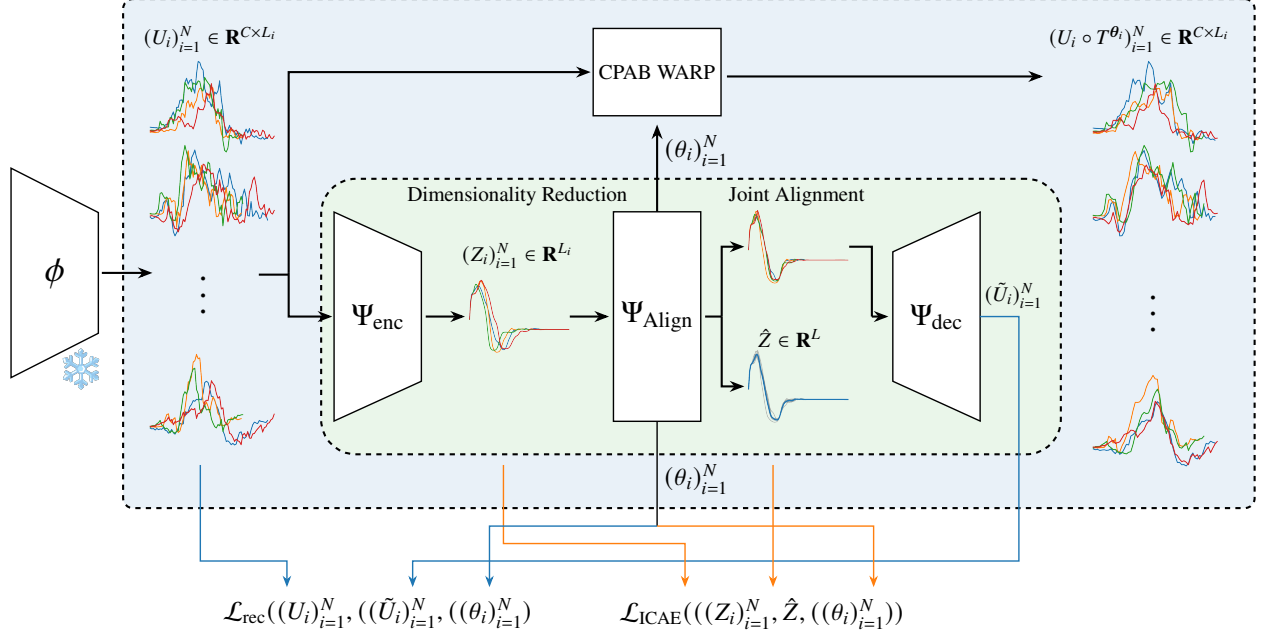


Figure 2. **Diffeomorphic Multitasking Autoencoder (D-MTAE)** for Temporal Prototype Learning, consists of: 1)  $\Psi_{\text{enc}}$ , an encoder for dimensionality reduction; 2)  $\Psi_{\text{Align}}$  [27], for joint alignment; and 3)  $\Psi_{\text{Dec}}$ , a decoder. The losses for JA and DR are  $\mathcal{L}_{\text{ICAE}}$  and  $\mathcal{L}_{\text{rec}}$  respectively. The feature extractor,  $\phi$ , could either be trained per dataset (e.g., CARL [2]) or a pretrained foundation model (e.g., DINO [1]).

**CPAB Transformations.** The CPAB (Continuous Piecewise Affine-Based) warp [9, 10] lies at the core of DTAN. Unlike discrete alignment approaches (e.g., DTW), a CPAB transformation is parameterized by a parameter vector  $\theta$  that defines a Continuous Piecewise Affine (CPA) velocity field,  $v^\theta$ , such that its integration yields a diffeomorphism (namely, a smooth, differentiable map, with a differentiable inverse),  $T^\theta$ . In the context of time series, this is a differentiable order-preserving time warp. This approach has three major advantages for learning-based alignment:

1. **Efficiency and Accuracy:** CPA velocity fields permit fast and accurate integration [9, 10], making them suitable for large-scale video data.
2. **Closed-Form Gradients:** The CPAB gradient,  $\nabla_\theta T^\theta$ , also admits a closed-form solution [16], which enables stable end-to-end training of neural alignment models.
3. **Invertibility and symmetry:** CPAB warps are invertible, where  $(T^\theta)^{-1} = T^{-\theta}$ . This is in contrast to DTW, which might produce different warping paths for  $\text{DTW}(X, Y)$  and  $\text{DTW}(Y, X)$ ,

Once a DTAN has been trained for a particular class of sequences, it can be applied directly to new data without re-solving an alignment objective from scratch, thus making the entire pipeline efficient for both training and inference.

### 3.2. Temporal Prototype Learning

**Architecture.** Given  $N$  videos depicting the same action and their high-dimensional embeddings,  $\{U_i\}_{i=1}^N$ , we seek

to learn a temporal prototype,  $\hat{U} \in \mathbb{R}^{C \times L}$  where  $L$  is the prototype’s length and  $C$  is the number of channels in the learned representation. Since  $\{U_i\}_{i=1}^N$  are misaligned, a simple averaging will result in a distorted average sequence that represents the data poorly. Another key insight is that while at each time  $t$ ,  $u_i^t \in \mathbb{R}^C$ , the  $(u_i^t)_{t=1}^{L_i}$  values (where  $L_i$  is the length of  $S_i$ , hence also of  $U_i$ ) should represent, in theory, phases in a 1D action progression. Thus, to learn temporal prototypes of action progression, a 1D representation should suffice. This is further motivated by the fact that the high-dimensional representation might hold irrelevant information, which hinders the alignment task. Taking the discussion above into consideration, we propose a *simultaneous dimensionality reduction and JA* to achieve a compact representation of the action and its progression.

Specifically, we introduce a novel Diffeomorphic Multitasking Autoencoder (D-MTAE; depicted in Figure 2) designed to learn dimensionality reduction and joint alignment. D-MTAE consists of: 1) an encoder,  $\Psi_{\text{encoder}} : \mathbb{R}^{C \times L_i} \rightarrow \mathbb{R}^{L_i}$ , that maps the  $C$ -dimensional embedding sequence,  $U_i \in \mathbb{R}^{C \times L_i}$ , into a latent 1D projection,  $Z_i \in \mathbb{R}^{L_i}$ ; 2) an alignment module,  $\Psi_{\text{Align}}$ , that performs JA on the latent representations,  $(Z_i)_{i=1}^N$ ; 3) a decoder model,  $\Psi_{\text{decoder}} : \mathbb{R}^{L_i} \rightarrow \mathbb{R}^{C \times L_i}$ , that maps the latent projection back to the original domain.

**Latent Representation Alignment Loss.** The encoder,  $\Psi_{\text{encoder}}$ , is a Temporal Convolutional Network (TCN) that maps each  $U_i$  to a univariate latent sequence  $Z_i \in \mathbb{R}^{L_i}$ .



The alignment module  $\Psi_{\text{Align}}$  predicts warping parameters  $\{\theta_i\}_{i=1}^N$  to produce time-warped latent signals  $\tilde{Z}_i = Z_i \circ T^{\theta_i}$ . We seek a shared prototype  $\hat{Z} \in \mathbb{R}^L$  that captures the common temporal progression across all videos. Building on the Inverse Consistency Averaging Error (ICAE) [26], which enables JA without explicit warp regularization, we minimize

$$\mathcal{L}_{\text{ICAE}} = \frac{1}{N} \sum_{i=1}^N \left\| \hat{Z} \circ T^{-\theta_i} - Z_i \right\|_{\ell_2}^2. \quad (3)$$

Since videos can vary greatly in length, we fix the length of  $\hat{Z}$  to be the *median* of all video lengths to prevent ‘collapse’ of the prototype (observed empirically when video lengths differ significantly). This approach robustly maintains an appropriate temporal scale in the aligned representation.

**Misalignment-Invariant Reconstruction Loss.** Ensuring that  $\hat{Z}$  accurately reflects the data’s true progression requires preventing trivial solutions (*e.g.*, collapsing each  $\tilde{Z}_i$  to a single repeated scalar). To address this, we include a decoder  $\Psi_{\text{decoder}}$  that reconstructs the original embeddings from the aligned latents, yielding  $\tilde{U}_i = \Psi_{\text{decoder}}(\tilde{Z}_i)$ . We then apply the inverse warp  $T^{-\theta_i}$  to  $\tilde{U}_i$  and measure the discrepancy from the original embeddings  $U_i$ :

$$\mathcal{L}_{\text{rec}} = \frac{1}{N} \sum_{i=1}^N \left\| U_i - \tilde{U}_i \circ T^{-\theta_i} \right\|_{\ell_2}^2. \quad (4)$$

This *misalignment-invariant* reconstruction encourages the prototype to capture meaningful temporal structure, as it must remain consistent when warped back to each video’s original timeline.

**Overall loss:** The overall loss function is obtained by combining the JA loss (Equation 3) and reconstruction loss (Equation 4)

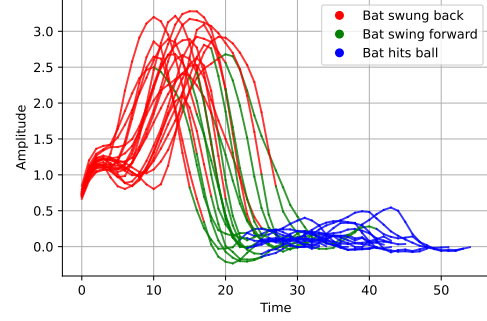
$$\mathcal{L}_{\text{TPL}} = \lambda_t \mathcal{L}_{\text{ICAE}} + \mathcal{L}_{\text{rec}} \quad (5)$$

where  $\lambda_t$  controls the ‘annealing’ of the alignment loss. This allows for faster and reliable convergence for the simultaneous learning of reconstruction and alignment. It is defined as

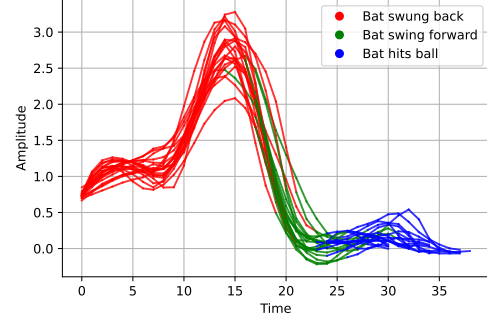
$$\lambda_t = \frac{1}{1 + e^{-\alpha(t-t_0)}} \quad (6)$$

where  $\alpha$  is a scaling factor (fixed at 2 for all experiments),  $t$  is the current training epoch, and  $t_0$  is the epoch at which  $\lambda_t$  reaches 1 and the annealing stops (set to  $\frac{N_{\text{epochs}}}{2}$ ).

The D-MTAE is trained simultaneously in an end-to-end fashion. We used PyTorch [18] for all of our experiments. The DIFW package [16] was used for the CPAB [9, 10] implementation. Both  $\Psi_{\text{encoder}}$  and  $\Psi_{\text{decoder}}$  are 3-layer TCNs. For  $\Psi_{\text{Align}}$  we follow [26] and use InceptionTime [13]. For a detailed description of the training procedure and hyperparameters, see our supplementary material (SupMat).



(a) Baseball swing learned 1D Latent representation.



(b) After synchronization.

Figure 3. Univariate representations learned by TPL for 20 videos depicting a *Baseball swing* colored by the phase labels, before (top) and after Synchronization (bottom).

### 3.3. Multiple Video Synchronization

Aligning new videos is achieved by first predicting the warping parameters for the latent representations,  $(\theta_i)_{i=1}^N$ , and applying them to the original videos; *i.e.*,  $(S_i \circ T^{\theta_i})_{i=1}^N$ . The temporal prototype is defined as the average of the representation of the aligned sequences:

$$\hat{U} \triangleq \frac{1}{N} \sum_{i=1}^N U_i \circ T^{\theta_i}. \quad (7)$$

Once the temporal prototypes are computed, we can transfer dense, frame-level, annotations from training to test data. This is achieved by first annotating the prototypes and then transferring their annotations to the test videos using temporal alignment. Formally, let  $(A_i)_{i=1}^N$  be the dense annotations of the input videos (*i.e.*,  $A_i$  is a sequence of length  $L_i$  where  $A_i[t]$  is the frame label at time step  $t$ ). To annotate the temporal prototype, we take the mode (*i.e.*, the most frequent label) of the *aligned* annotations at time step  $t$ ,  $(A_i \circ T^{\theta_i})[t]$ . The prototype labels,  $\hat{A}$ , for each time step are defined as

$$\hat{A}[t] \triangleq \text{mode}(\mathcal{A}[t]) \quad (8)$$

where  $\mathcal{A}[t] = ((A_i \circ T^{\theta_i})[t])_{i=1}^N$  are all labels at time step  $t$  after alignment. New videos are annotated by aligning them to their corresponding class prototype and using the matching

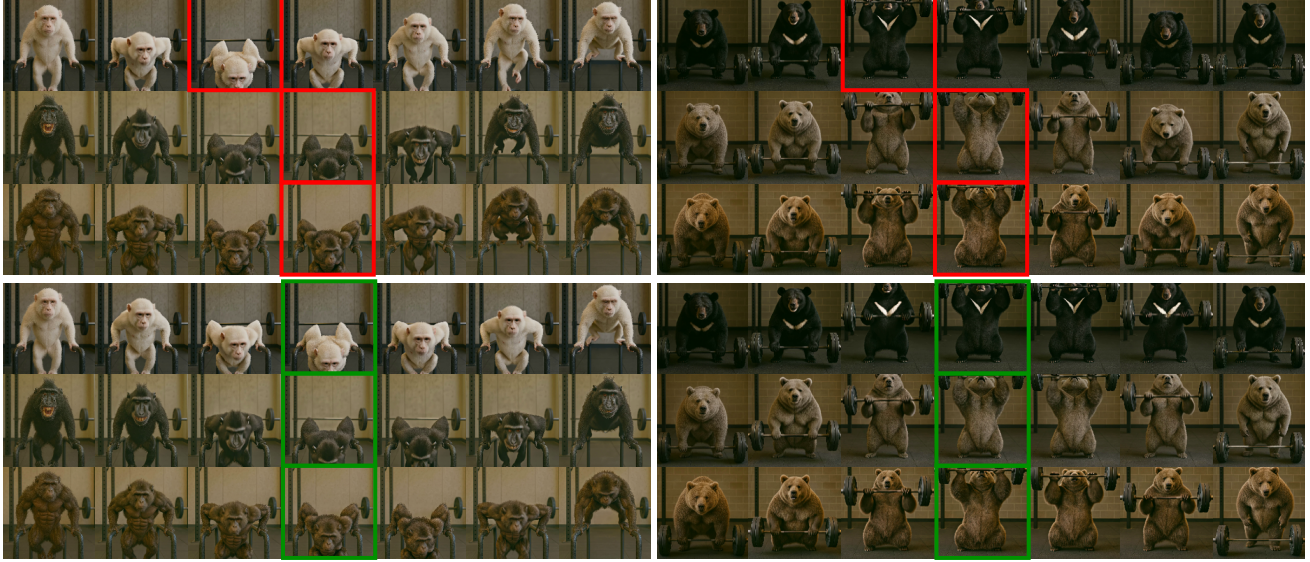


Figure 4. Examples from our GenerativeAI Multiple Video Synchronization (GenAI-MVS) dataset, showing seven equally spaced frames before (top) and after (bottom) synchronization. The first video (left) depicts a “monkey doing dips,” and the second video (right) shows a “bear performing a deadlift.” We highlight mismatches in the original videos in red, and TPL matching in green. In both cases, alignment via TPL successfully synchronizes the key phases of the action progression.

frame labels. Figure 3 shows the 1D representations colored by the ground-truth annotations of a 20 *Baseball swing* videos [33] before and after synchronization.

### 3.4. Limitations

TPL’s effectiveness is intricately tied to the quality of the initial features, *i.e.*, the initial embeddings used. Should these embeddings be of poor quality or fail to adequately represent the data, the resulting outcomes may be suboptimal.

## 4. Results

In this section, we present a series of experiments designed to demonstrate the effectiveness of TPL for multiple video synchronization (MVS).

### 4.1. Datasets

We evaluate TPL on the following datasets:

1. **Pouring** [24]: A standard benchmark consisting of 84 videos of people pouring liquids into glasses.
2. **Penn Action** [33]: This dataset contains 2326 videos of 15 different actions performed in the wild, varying in camera angles, lighting, action duration, backgrounds, and subjects, with phase-level annotations produced by [8].
3. **Internet Video Dataset** [7]: A smaller dataset, similar to Penn Action, comprising 124 videos of 20 actions. We annotate the phases in the same manner as [8].
4. **GenAI Multiple Video Synchronization Dataset**: We introduce a first-of-its-kind collection of AI-generated videos using KlingAI for the task of MVS (GenAI-MVS).

For each action, a text prompt is composed, and an initial image is generated using ChatGPT. The image and prompt are then used as input to Kling AI to generate a video of the action. Multiple videos of the same action are generated in this manner, resulting in natural variation in both visual appearance and temporal execution. The dataset contains 5 classes and 82 hand-picked videos curated for MVS, each accompanied by phase progression annotations (see **SupMat** for more details).

### 4.2. Evaluation Metrics

As stated in [6], existing benchmarks often rely on proxy tasks such as phase classification by a linear classifier or Kendall’s Tau for phase progression [8]. These metrics had been shown to be affected by spurious correlations between the positional encoding of the model (*e.g.*, CARL [2]) and the phase labels. To evaluate alignment directly, we follow [6] and introduce two metrics: *Cycle-Back Consistency (CBC)*, which measures how well phase labels are preserved when warping videos to the prototype and then un-warping them back, and *Phase Label Propagation (PLP)*, which measures alignment quality by transferring phase labels from a train-set prototype to test videos. We still report phase classification and Kendall’s Tau for completeness, but CBC and PLP offer a clearer measure of real-world alignment performance:

- **Cycle-Back Consistency (CBC)**. Measures how well the prototype maintains phase information. The videos are warped to the prototype and label it according to their annotation. The prototype is then unwarped back to each

Table 2. Comparison of different features and alignment methods on Penn Action, Internet Videos, and Gen AI. We report the alignment objective to minimize (Obj.), Cycle-Back Consistency (CBC), Phase Label Propagation (PLP), and total runtime (Time) in seconds.

|                               |                               |            |                     | Penn Action  |              |       | Internet Videos |              |      | GenAI-MVS    |              |       |
|-------------------------------|-------------------------------|------------|---------------------|--------------|--------------|-------|-----------------|--------------|------|--------------|--------------|-------|
| Features                      | Method                        | Obj.       |                     | CBC          | PLP          | Time  | CBC             | PLP          | Time | CBC          | PLP          | Time  |
| CARL<br>+ dataset training    | Baseline                      | Euc.       | Euc.                | 0.621        | 0.607        | 0.65  | N/A             | N/A          | N/A  | N/A          | N/A          | N/A   |
|                               |                               | DTAN       | WCSS                | 0.42         | 0.415        | 588   | N/A             | N/A          | N/A  | N/A          | N/A          | N/A   |
|                               |                               | DTAN       | WCSS + Reg.         | 0.647        | 0.625        | 710   | N/A             | N/A          | N/A  | N/A          | N/A          | N/A   |
|                               |                               | DTAN       | ICAE                | 0.773        | 0.765        | 579   | N/A             | N/A          | N/A  | N/A          | N/A          | N/A   |
|                               |                               | DBA        | DTW                 | 0.947        | 0.925        | 2345  | N/A             | N/A          | N/A  | N/A          | N/A          | N/A   |
|                               |                               | SoftDTW    | SoftDTW             | 0.944        | 0.926        | 978   | N/A             | N/A          | N/A  | N/A          | N/A          | N/A   |
|                               |                               | TPL (ours) | $\mathcal{L}_{TPL}$ | <b>0.962</b> | <b>0.939</b> | 482   | N/A             | N/A          | N/A  | N/A          | N/A          | N/A   |
| DINO-ViT<br>(“off-the-shelf”) |                               | DTAN       | WCSS                | 0.418        | 0.419        | 599   | 0.712           | 0.63         | 215  | 0.759        | 0.768        | 105   |
|                               |                               | DTAN       | WCSS + Reg.         | 0.591        | 0.604        | 707   | 0.764           | 0.647        | 224  | 0.762        | 0.752        | 110   |
|                               |                               | DTAN       | ICAE                | 0.572        | 0.578        | 639   | 0.874           | 0.683        | 232  | 0.833        | 0.740        | 114   |
|                               |                               | DBA        | DTW                 | 0.756        | 0.773        | 5415  | 0.882           | 0.871        | 25   | 0.886        | 0.906        | 62    |
|                               |                               | SoftDTW    | SoftDTW             | 0.750        | 0.777        | 3010  | 0.883           | 0.872        | 53   | 0.890        | 0.908        | 58    |
|                               |                               | TPL (ours) | $\mathcal{L}_{TPL}$ | <b>0.788</b> | <b>0.803</b> | 534   | <b>0.912</b>    | <b>0.907</b> | 112  | <b>0.953</b> | <b>0.933</b> | 108   |
|                               | OpenCLIP<br>(“off-the-shelf”) |            | DTAN                | WCSS         | 0.418        | 0.419 | 629             | 0.792        | 0.7  | 223          | 0.834        | 0.803 |
|                               |                               | DTAN       | WCSS + Reg.         | 0.636        | 0.615        | 736   | 0.83            | 0.742        | 229  | 0.754        | 0.748        | 112   |
|                               |                               | DTAN       | ICAE                | 0.704        | 0.688        | 680   | 0.858           | 0.742        | 237  | 0.535        | 0.614        | 110   |
|                               |                               | DBA        | DTW                 | 0.807        | 0.808        | 4692  | 0.885           | 0.842        | 33   | 0.918        | 0.929        | 63    |
|                               |                               | SoftDBA    | SoftDTW             | 0.859        | 0.831        | 1882  | 0.901           | 0.833        | 34   | 0.926        | 0.921        | 68    |
|                               |                               | TPL (ours) | $\mathcal{L}_{TPL}$ | <b>0.873</b> | <b>0.857</b> | 587   | <b>0.916</b>    | <b>0.902</b> | 146  | <b>0.942</b> | <b>0.946</b> | 115   |

video, and the phase labels are compared. A higher CBC indicates more accurate and robust synchronization.

- **Phase Label Propagation (PLP).** Assesses alignment by transferring phase labels from a prototype to each test video. The better the alignment, the more accurately these labels will map onto the correct frames in the test video. PLP thus serves as a direct measure of alignment quality.
- **Phase Classification Accuracy.** Assess the embedding quality by training a linear classifier on the per-frame embedding to predict the phase labels.
- **Kendall’s Tau.** A rank-correlation metric that evaluates the chronological order of phases across videos.

### 4.3. Comparison with Multiple Sequence Alignment (MSA) Methods

To evaluate our method’s performance w.r.t. existing approaches, we align sets of videos depicting the same action using TPL and compare the results against 4 representative MSA methods: Euclidean baseline (Euc.), where we zero-pad all videos to have the same length (according to the longest one) and compute metrics only on each video’s valid regions. DBA [19], SoftDBA [4], and DTAN [27]. DBA and SoftDBA are optimization-based methods set to minimize the DTW and SoftDTW from the average sequence, respectively. For SoftDTW, we report the best results among  $\gamma \in [0.01, 0.1, 1]$ . DTAN is a learning-based method that predicts CPAB [9] warps to minimize the JA loss. We evaluate DTAN with three losses: Within-Class Sum of Squares (WCSS), WCSS + Regularization (WCSS+Reg.), and the current state-of-the-art in time series averaging, DTAN+ICAE [26]. All DTAN models were trained using the closed-form CPAB gradient [16]. We evaluate frame-level embedding from three feature extractors: 1) CARL [2], a video transformer that requires per-dataset

training, 2) DINO-ViT-v2 [17], a pre-train image transformer where we use the per-frame CLS token as the embedding, and 3) OpenCLIP [3], an open-source, more recent variation of CLIP [21]. We note that the available video foundation models (e.g., VideoMAE [30]) do not produce a per-frame embedding vector and were therefore excluded from this evaluation. We report CBC, LPL, and total runtime (training and inference time) on the Penn [33], Internet Videos [7], and GenAI-MVS datasets.

The results are presented in Table 2. We have found that internet videos [7] and GenAI-MVS did not have enough data to train CARL properly and are thus omitted. We observe that TPL significantly outperforms all DTAN variants over all datasets and feature extractors. As discussed in § 3.1, current DTAN formulations are ill-equipped to handle the real-world video embeddings. TPL also outperforms DBA and SoftDBA across all benchmarks. While the margin in performance is less significant compared with DTAN, **TPL total runtime is 10 times faster** than DBA and 4 – 5 than SoftDBA on the largest dataset, Penn Action [33]. GenAI-MSV results are further discussed in § 4.6.

### 4.4. Prototype-aligned Features

To determine whether TPL prototypes capture meaningful phase progression, we evaluate phase classification accuracy and Kendall’s Tau rank correlation on the videos *after* they have been aligned to the common prototype. By warping each video to the TPL prototype, we test whether these aligned representations provide more discriminative features for recognizing action phases. We conduct these experiments on both Penn Action [33] and Pouring [25] datasets. We compare the prototyped-aligned features to standard benchmarks in video representation learning: TCC [8], GTA [11]



, LAV [12], VAVA [15], VSP [32], and CARL[2]. We report the results from their respective papers. The results, presented in Table 3, indicates that TPL-aligned representations are on-par with VSP and CARL, the two strongest baselines. As mentioned in § 4.2, these metrics are not ideal for assessing alignment quality. However, these findings indicate that the synchronized embeddings retain their temporal information after alignment.

Table 3. Phase classification accuracy (Acc.) & Kendall’s Tau ( $\tau$ ). Positional embedding is indicated (Pos. Emb.).

| Pos. Emb. | Method     | Penn Action  |              | Pouring      |              |
|-----------|------------|--------------|--------------|--------------|--------------|
|           |            | Acc.         | $\tau$       | Acc.         | $\tau$       |
| ✗         | TCC [8]    | 74.39        | 0.623        | 86.14        | 0.670        |
| ✗         | GTA [11]   | 78.90        | 0.654        | 85.16        | 0.750        |
| ✗         | LAV [12]   | 78.68        | 0.805        | 92.84        | 0.856        |
| ✗         | VAVA [15]  | 84.48        | 0.805        | 92.84        | 0.875        |
| ✓         | VSP [32]   | 93.12        | 0.986        | 93.85        | 0.990        |
| ✓         | CARL [2]   | 93.07        | 0.985        | 93.73        | 0.992        |
| ✓         | TPL (ours) | <b>93.31</b> | <b>0.990</b> | <b>93.88</b> | <b>0.993</b> |

#### 4.5. Frame Retrieval Efficiency

TPL’s MVS facilitates faster frame retrieval than standard KNN frame-retrieval approach, where each frame from each test video is compared to all frames in all videos in the train set. This implies  $O(N_{\text{train}}N_{\text{test}}L^2)$  (assuming fixed-length  $L$  for simplicity). In contrast, video synchronization allows this process to be linear in  $L$ . This advantage arises because TPL establishes a single temporal reference for the action progression, allowing for direct frame lookup at each time step. For evaluation, we perform 1-NN frame retrieval on Penn using CARL’s embedding and report the phase classification accuracy and runtime (including inference time for TPL). As shown in Table 4, performing frame retrieval only between synchronized frames is **125 times faster** than a full KNN search (0.24 [sec] and 30 [sec], respectively).

#### 4.6. Generalizing to Generative AI Videos

Beyond real-world footage, we also study the effectiveness of TPL on synthetic videos generated via a combination of ChatGPT and KlingAI. For each action category, we compose a detailed text prompt and generate an initial reference image using ChatGPT. This image and prompt are then used as input to KlingAI to produce a video illustrating the target action. Finally, we annotate the phase progression in each video similarly to [8]. A key challenge in creating this dataset was identifying videos suitable for MVS. Current video generators often produce truncated action progressions, omit essential phases, or generate clips that do not depict the intended action. After filtering out problematic samples, we retained a diverse set of videos that still pose realistic alignment challenges.

An example of AI-generated video synchronization via TPL is shown in Figure 4. We display seven equally spaced

Table 4. Unsynchronized vs. synchronized Nearest-neighbor frame retrieval comparison on Penn Action.

| Method              | Complexity                              | Time (sec)  |
|---------------------|---|-------------|
| Unsynchronized      | $O(N_{\text{train}}N_{\text{test}}L^2)$ | 30.1        |
| synchronized (Ours) | $O(N_{\text{train}}N_{\text{test}}L)$   | <b>0.24</b> |

Table 5. Ablation study evaluation on Penn Action.

| Condition                       | CBC   | PLP   |
|---------------------------------|-------|-------|
| Baseline (Euclidean)            | 64.6% | 63.5% |
| No 1D Bottleneck                | 80.4% | 81.5% |
| Encoder Only                    | 56.5% | 51.3% |
| + Decoder, Standard ICAE        | 97.3% | 96.7% |
| + ICAE with Median Length (TPL) | 100%  | 100%  |

frames taken from the original (top) and synchronized (bottom) sequences. For instance, in the “Bear deadlift” example, TPL successfully aligns key motion phases, including the moment the bear begins lifting and reaches the upright position, demonstrating improved temporal coherence. We also report the CBC and PLP for the MSA methods and report them in Table 2. TPL achieves higher CBC and Phase Label Propagation PLP than traditional Soft/DBA and DTAN. These results highlight the ability of TPL to extend beyond conventional, human-recorded video sources to the emerging domain of AI-generated content, providing a robust solution for synchronizing multiple generative clips depicting the same action.

#### 4.7. Ablation Study

Table 5 shows the ablation study for Penn Action using the Euclidean distance as a baseline. Only using the alignment network (without the 1D bottleneck) yields improvement in both CBC and PLP. However, introducing only the encoder diminishes the performance significantly, indicating the importance of reconstruction for stable training, as seen by the significant improvement in results when using the decoder. Finally, enforcing a median-length prototype gives the full TPL framework that achieves the best overall results.

### 5. Conclusion

We introduced **Temporal Prototype Learning (TPL)**, a novel framework for synchronizing multiple videos from different scenes without relying on a reference by simultaneously reducing high-dimensional embeddings to a univariate representation. TPL outperforms existing alignment methods on a range of real-world datasets, while also generalizing effectively to AI-generated content exhibiting diverse visual styles and timing variations. Moreover, its prototype-based alignment yields faster frame retrieval and requires fewer pairwise comparisons, making TPL well-suited for large-scale video analytics.



## Acknowledgments

This work was supported by the Lynn and William Frankel Center at BGU CS, by the Israeli Council for Higher Education via the BGU Data Science Research Center, and by Israel Science Foundation Personal Grant #360/21. R.S.W.'s work was supported by the Kreitman School of Advanced Graduate Studies.

## References

- [1] Mathilde Caron, Hugo Touvron, Ishan Misra, Hervé Jégou, Julien Mairal, Piotr Bojanowski, and Armand Joulin. Emerging properties in self-supervised vision transformers. In *Proceedings of the IEEE/CVF international conference on computer vision*, pages 9650–9660, 2021. [2](#), [3](#), [4](#)
- [2] Minghao Chen, Fangyun Wei, Chong Li, and Deng Cai. Frame-wise action representations for long videos via sequence contrastive learning. In *CVPR*, 2022. [1](#), [2](#), [3](#), [4](#), [6](#), [7](#), [8](#)
- [3] Mehdi Cherti, Romain Beaumont, Ross Wightman, Mitchell Wortsman, Gabriel Ilharco, Cade Gordon, Christoph Schuhmann, Ludwig Schmidt, and Jenia Jitsev. Reproducible scaling laws for contrastive language-image learning. In *Proceedings of the IEEE/CVF conference on computer vision and pattern recognition*, pages 2818–2829, 2023. [2](#), [7](#)
- [4] Marco Cuturi and Mathieu Blondel. Soft-dtw: a differentiable loss function for time-series. *arXiv preprint arXiv:1703.01541*, 2017. [2](#), [7](#)
- [5] Hoang Anh Dau, Anthony Bagnall, Kaveh Kamgar, Chia Michael Yeh, Yan Zhu, Shaghayegh Gharghabi, Chotirat Ann Ratanamahatana, and Eamonn Keogh. The ucr time series archive. *IEEE/CAA Journal of Automatica Sinica*, 2019. [3](#)
- [6] Ishan Rajendrakumar Dave, Fabian Caba Heilbron, Mubarak Shah, and Simon Jenni. Sync from the sea: retrieving alignable videos from large-scale datasets. In *European Conference on Computer Vision*, pages 371–388. Springer, 2024. [6](#)
- [7] Junting Dong, Qing Shuai, Yuanqing Zhang, Xian Liu, Xiaowei Zhou, and Hujun Bao. Motion capture from internet videos. In *Computer Vision—ECCV 2020: 16th European Conference, Glasgow, UK, August 23–28, 2020, Proceedings, Part II 16*, pages 210–227. Springer, 2020. [6](#), [7](#)
- [8] Debidatta Dwibedi, Yusuf Aytar, Jonathan Tompson, Pierre Sermanet, and Andrew Zisserman. Temporal cycle-consistency learning. In *CVPR*, 2019. [1](#), [2](#), [6](#), [7](#), [8](#)
- [9] Oren Freifeld, Søren Hauberg, Kayhan Batmanghelich, and John W. Fisher III. Highly-expressive spaces of well-behaved transformations: Keeping it simple. In *ICCV*, 2015. [2](#), [3](#), [4](#), [5](#), [7](#)
- [10] Oren Freifeld, Søren Hauberg, Kayhan Batmanghelich, and John W. Fisher III. Transformations based on continuous piecewise-affine velocity fields. *IEEE TPAMI*, 2017. [2](#), [3](#), [4](#), [5](#)
- [11] Isma Hadji, Konstantinos G Derpanis, and Allan D Jepson. Representation learning via global temporal alignment and cycle-consistency. In *CVPR*, 2021. [2](#), [7](#), [8](#)
- [12] Sanjay Haresh, Sateesh Kumar, Huseyin Coskun, Shahram N Syed, Andrey Konin, Zeeshan Zia, and Quoc-Huy Tran. Learning by aligning videos in time. In *CVPR*, 2021. [2](#), [8](#)
- [13] Hassan Ismail Fawaz, Benjamin Lucas, Germain Forestier, Charlotte Pelletier, Daniel F Schmidt, Jonathan Weber, Geoffrey I Webb, Lhassane Idoumghar, Pierre-Alain Muller, and François Petitjean. Inceptiontime: Finding alexnet for time series classification. *Data Mining and Knowledge Discovery*, 2020. [5](#)
- [14] Junwei Liang, Poyao Huang, Jia Chen, and Alexander Hauptmann. Synchronization for multi-perspective videos in the wild. In *2017 IEEE International Conference on Acoustics, Speech and Signal Processing (ICASSP)*, pages 1592–1596. IEEE, 2017. [2](#)
- [15] Weizhe Liu, Bugra Tekin, Huseyin Coskun, Vibhav Vineet, Pascal Fua, and Marc Pollefeys. Learning to align sequential actions in the wild. In *CVPR*, 2022. [1](#), [2](#), [8](#)
- [16] Iñigo Martinez, Elisabeth Viles, and Igor G Olaizola. Closed-form diffeomorphic transformations for time series alignment. In *ICML*. PMLR, 2022. [2](#), [3](#), [4](#), [5](#), [7](#)
- [17] Maxime Oquab, Timothée Darcet, Théo Moutakanni, Huy Vo, Marc Szafraniec, Vasil Khalidov, Pierre Fernandez, Daniel Haziza, Francisco Massa, Alaaeldin El-Nouby, et al. Dinov2: Learning robust visual features without supervision. *arXiv preprint arXiv:2304.07193*, 2023. [7](#)
- [18] Adam Paszke, Sam Gross, Francisco Massa, Adam Lerer, James Bradbury, Gregory Chanan, Trevor Killeen, Zeming Lin, Natalia Gimelshein, Luca Antiga, et al. Pytorch: An imperative style, high-performance deep learning library. *NeurIPS*, 2019. [5](#)
- [19] François Petitjean, Alain Ketterlin, and Pierre Gançarski. A global averaging method for dynamic time warping, with applications to clustering. *Pattern Recognition*, 2011. [2](#), [7](#)
- [20] François Petitjean, Germain Forestier, Geoffrey I Webb, Ann E Nicholson, Yanping Chen, and Eamonn Keogh. Dynamic time warping averaging of time series allows faster and more accurate classification. In *IEEE ICDM*, 2014. [2](#)
- [21] Alec Radford, Jong Wook Kim, Chris Hallacy, Aditya Ramesh, Gabriel Goh, Sandhini Agarwal, Girish Sastry, Amanda Askell, Pamela Mishkin, Jack Clark, et al. Learning transferable visual models from natural language supervision. In *International conference on machine learning*, pages 8748–8763. PMLR, 2021. [7](#)
- [22] H. Sakoe. Dynamic-programming approach to continuous speech recognition. *The International Congress of Acoustics*, 1971. [2](#)
- [23] H. Sakoe and S. Chiba. Dynamic programming algorithm optimization for spoken word recognition. *IEEE TASSP*, 1978. [2](#)
- [24] Pierre Sermanet, Corey Lynch, Jasmine Hsu, and Sergey Levine. Time-contrastive networks: Self-supervised learning from multi-view observation. *CoRR*, abs/1704.06888, 2017. [6](#)
- [25] Pierre Sermanet, Corey Lynch, Yevgen Chebotar, Jasmine Hsu, Eric Jang, Stefan Schaal, Sergey Levine, and Google Brain. Time-contrastive networks: Self-supervised learning from video. In *ICRA*. IEEE, 2018. [7](#)
- [26] Ron Shapira Weber and Oren Freifeld. Regularization-free diffeomorphic temporal alignment nets. In *ICML*. PMLR, 2023. [2](#), [3](#), [5](#), [7](#)

- [27] Ron Shapira Weber, Matan Eyal, Nicki Skaftø Detlefsen, Oren Shriki, and Oren Freifeld. Diffeomorphic temporal alignment nets. In *NeurIPS*, 2019. [2](#), [3](#), [4](#), [7](#)
- [28] Prarthana Shrestha, Mauro Barbieri, and Hans Weda. Synchronization of multi-camera video recordings based on audio. In *Proceedings of the 15th ACM international conference on Multimedia*, pages 545–548, 2007. [2](#)
- [29] Jake Snell, Kevin Swersky, and Richard Zemel. Prototypical networks for few-shot learning. *NeurIPS*, 2017. [2](#)
- [30] Zhan Tong, Yibing Song, Jue Wang, and Limin Wang. Videomae: Masked autoencoders are data-efficient learners for self-supervised video pre-training. *Advances in neural information processing systems*, 35:10078–10093, 2022. [7](#)
- [31] Oliver Wang, Christopher Schroers, Henning Zimmer, Markus Gross, and Alexander Sorkine-Hornung. Videosnapping: Interactive synchronization of multiple videos. *ACM Transactions on Graphics (TOG)*, 33(4):1–10, 2014. [2](#)
- [32] Heng Zhang, Daqing Liu, Qi Zheng, and Bing Su. Modeling video as stochastic processes for fine-grained video representation learning. In *CVPR*, 2023. [1](#), [8](#)
- [33] Weiyu Zhang, Menglong Zhu, and Konstantinos G Derpanis. From actemes to action: A strongly-supervised representation for detailed action understanding. In *ICCV*, 2013. [2](#), [6](#), [7](#)